Communications

Line Patterns in the Mosaic Electrical Properties of Human Skin—A Cross-Correlation Study

Ørjan G. Martinsen*, Sverre Grimnes, Lars Mørkrid, and Morten Hareide

***Abstract*—A vehicle with 16 electrodes for the two-dimensional electrical admittance mapping of human skin is presented. Measurements on 20 test subjects have been carried out and analyzed for the possible detection of line patterns in the electrical properties of the skin, claimed to coincide with the so-called acupuncture meridian lines of ancient Chinese medicine. No such lines were found.**

***Index Terms*—Electrical admittance, line patterns, low resistance points, meridians, skin.**

I. Introduction

The electrical properties of human skin are largely dependent of body part, environmental conditions and measuring system [1], [2]. The variations are extensive not only between body parts, however, but also within a smaller area on the skin. Various instruments for small area electrical measurements have been presented, based on e.g., roller electrodes [3] and a suction microelectrode [4].

In this paper, we present an instrument and an electrode system for skin admittance scans with a resolution of 1 mm in two dimensions. The system has been developed for the investigation of local variations in skin admittance, including the mapping of so-called "low impedance" or "low resistance" points. Furthermore, lines characterized by a thinner epidermis and, thus, low impedance are claimed to exist in the skin. The about 1-mm-wide lines are supposed to coincide with the "meridian lines" of ancient Chinese medicine, and are reported to be detectable by means of electrical measurements [5]–[8]. Meridian lines along the volar side of the arm according to Zhu and Hao [5], are shown in Fig. 1. We, thus, wanted to investigate whether any such pattern could be detected by electrical measurements.

II. Methods

An electrode vehicle with an array of 16 resilient steel electrodes has been constructed (Fig. 2). A layer of isolating lacquer was applied to each electrode and the tips of the electrodes were then honed in order to achieve a uniform, pressure independent contact area of approx. 0.25 mm^2 (0.5 mm $\times$ 0.5 mm). The center-distance between two electrodes is 1 mm. When the two vehicle rollers are in contact with the skin, the electrodes are applied with a pressure of about 15 g/mm^2. A large gel-electrode is used as a counter electrode to the 16 measuring electrodes in a two-electrode system.

Manuscript received October 13, 2000; revised March 5, 2001. *Asterisk indicates corresponding author.*

*Ø. G. Martinsen is with the Department of Physics, University of Oslo, POB 1048 Blindern, N-0316 Oslo, Norway (e-mail: ogm@fys.uio.no).

S. Grimnes is with the Department of Clinical and Biomedical Engineering, Rikshospitalet, N-0027 Oslo, Norway, and also with the Department of Physics, University of Oslo, Blindern, N-0316 Oslo, Norway.

L. Mørkid is with the Department of Clinical Chemistry, Rikshospitalet, N-0027 Oslo, Norway.

M. Hareide is with the Department of Physics, University of Oslo, Blindern, N-0316 Oslo, Norway.

Publisher Item Identifier S 0018-9294(01)04169-6.

Fig. 1. Meridian lines along the volar side of the arm, according to Zhu and Hao [5].

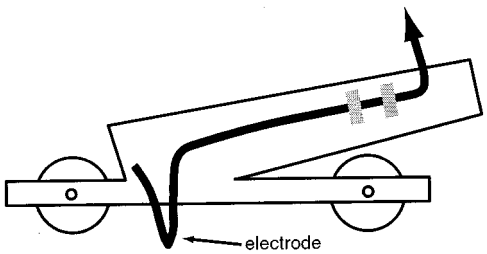

Fig. 2. Electrode vehicle.

The electrodes are periodically scanned through a multiplexer during movement of the vehicle, and the results are split into conductance and susceptance by means of phase sensitive detectors, and monitored through 12-bit analog-to-digital converters with a data acquisition program on a PC (Fig. 3). The scans are triggered manually each time the vehicle is moved 1 mm. A 418-Hz 100-mV root mean square measuring voltage was used, giving current densities well below the limit of linearity for the skin [9]. Using a low frequency will ensure that the measurements are focused on the epidermis [10], [11]. The polarization impedance is assumed to be significantly lower than the skin impedance [12], [13].

Measurements were performed on 20 Caucasian volunteers, ten females and ten males. Mean age was 29 (21–33) years, ambient temperature was 22 °C to 24 °C and air relative humidity was 24%–29%. They rested for 15 min before measurements were taken on the volar

0018–9294/01$10.00 © 2001 IEEE

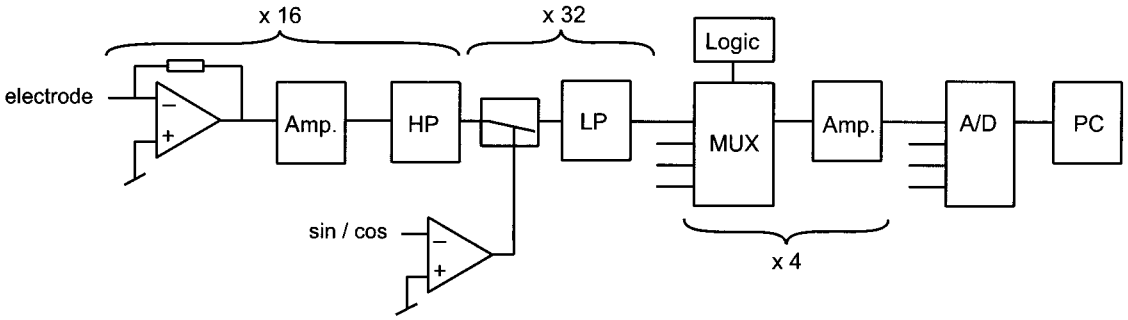

Fig. 3. Block diagram showing the measuring system. Number of parallel elements is indicated.

side of the left underarm. Lines were marked parallel to the forearm axis on the outer limits of the little finger and thumb sides of the volar underarm, and a point was marked midway between these lines and located 2/3 from the wrist toward the elbow. Four measuring series were done on each person.

1) Vehicle dragged in lateral direction on anterior facing volar underarm from little finger line and 3/4 toward the thumb line, mid electrode crossing the marked point.
2) Vehicle moved back in the opposite direction.
3) Vehicle dragged in $+45^\circ$ on lateral direction from little finger line and 3/4 toward the thumb line, mid electrode crossing the marked point.
4) Likewise in -45° on lateral direction.

The test person rested for 5 min between each of the four measuring series.

As a common trend of increasing admittance values in the lateral direction on the underarm was found in all data series, a second-order trend removal was performed on all data before further statistical analysis. A cross-correlation analysis was performed between measurements on all neighboring electrodes to detect possible line patterns in the measured data. In each analysis between two electrodes, the number of lags between -5 and $+5$ where the highest coefficient of correlation was found, was recorded, and these recordings were grouped according to the four different directions of the measuring series. Here, "lag" means that the measured value of one electrode is not compared with that of the neighboring electrode from the same scan, but from an earlier or later scan according to the number of lags. Hence, a lag of $+2$ means that e.g., the measured value from electrode number 1 is compared with the value from electrode number 2 measured two scans ($=2$ mm) later.

As an example, Fig. 4 shows the results from susceptance measurements in direction 1 for one test subject. Only 10 electrodes are shown for clarity. The same data after trend removal are shown in Fig. 5.

Removing a third-order trend or a trend based on moving average, or analyzing the discrete derivative of the data, gave almost identical results.

To verify that the system was able to detect a line of higher admittance in the data, an artificial line was introduced in the susceptance data for direction 4, in the following way: The overall standard deviation (SD) of the measured susceptance was first calculated for all 20 scans in this direction after removal of the trend. Then, $2\times$SD was added to one measured value for each electrode in all 20 data sets, shifted 1 mm from electrode to electrode and starting at distance 20 mm from start. This would then simulate a line of $2\times$ SD higher susceptance running between the wrist and elbow on all test subjects, and should produce an increase in the number of cross-correlation maxima at lag 1.

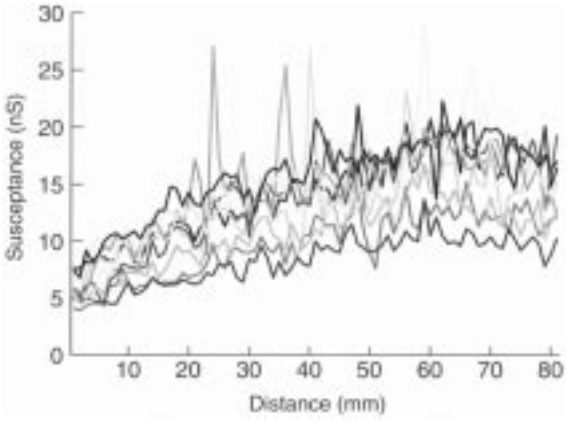

Fig. 4. Measured susceptance in direction 1 for one test subject. Before removal of trend.

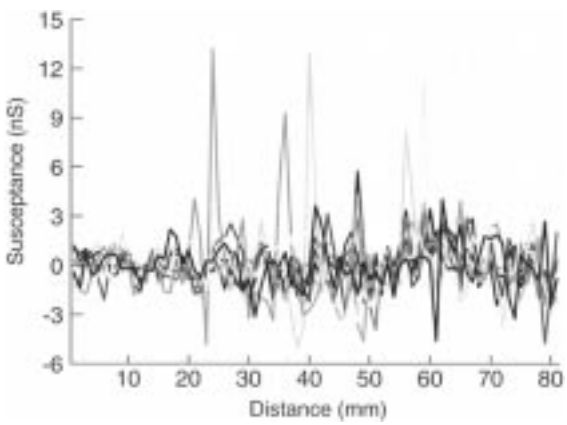

Fig. 5. Measured susceptance in direction 1 for one test subject. After removal of trend.

III. Results

Any line patterns in the measured conductance or susceptance should appear as a higher number of recordings for a specific lag in the total set of data from the same measured direction on different test subjects. In other words, when e.g., moving the vehicle in orthogonal direction to a low impedance line in the skin, lag 0 should in most cases have the highest cross-correlation value when separately analyzing all pairs of neighboring electrodes. Furthermore, an increase e.g., in recorded numbers of lag 0 for measurements in the lateral direction should be accompanied by a corresponding increase in the recorded number of lags -1 or $+1$ for measurements conducted $\pm 45^\circ$ on the lateral direction.

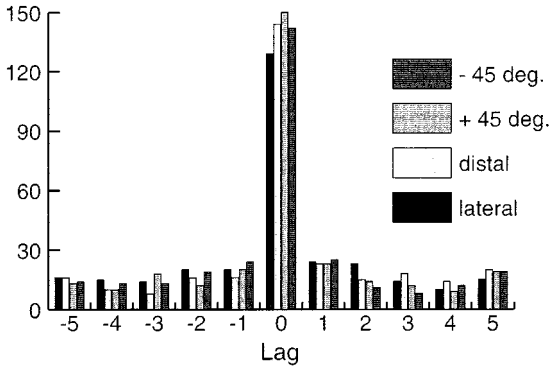

Fig. 6. Number of cross-correlation maxima found in the conductance measurements at different lags and for different direction of vehicle movement.

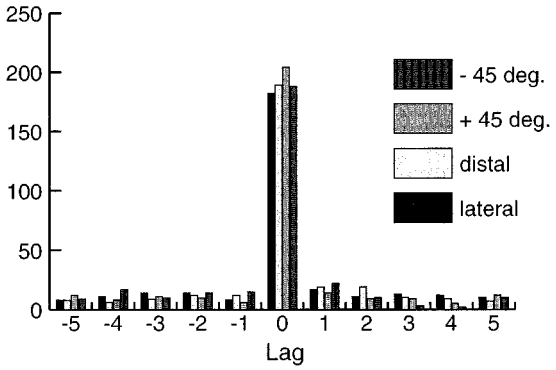

Fig. 7. Number of cross-correlation maxima found in the susceptance measurements at different lags and for different direction of vehicle movement.

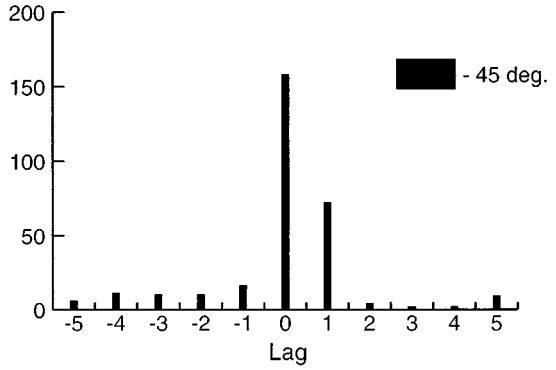

Fig. 8. Number of cross-correlation maxima found in the susceptance measurements at different lags for vehicle movement in -45° on lateral direction, after introducing an artificial line in the data.

The total numbers of correlation maxima found for the different lags when analyzing the conductance measurements are presented in Fig. 6 and for the susceptance measurements in Fig. 7. It was found that a significant higher number of correlation maxima were recorded for lag 0 in all the four directions, but no increase was found at lag -1 or $+1$ for the measurements conducted $\pm 45^\circ$ on the lateral direction. The results from the artificial line simulated in the susceptance data, are shown in Fig. 8.

IV. Discussion

A significantly higher number of cross-correlation maxima was found only for lag 0 in this study, and since this was not accompanied by a maximum at ± 1 for measurements conducted $\pm 45^\circ$ on lateral direction, this is interpreted as being due to the measuring system itself, and most likely caused by unsteady movement of the vehicle. Introducing a $2 \times$ SD artificial increase in the susceptance data for movement -45° on lateral direction, gave a unambiguous increase in the number of cross-correlation maxima at lag 1, and it is obvious from Fig. 8 that the system is able to detect the artificial line introduced in the measured data. Furthermore, a series of experiments were performed where a line was either lightly scratched in the skin or produced by applying a woollen thread soaked in tap water or saline for 1 min on the skin. In the latter case, the skin was wiped dry before the measurements were conducted. In all these experiments, the increase in conductance or susceptance found on these lines represented more than $6 \times$ SD relative to the baseline. This was taken as a clear indication of the system's ability to detect even relatively small changes in the electrical properties of the skin, and verifies that the system would have been able to reveal any line patterns of significantly increased electrical admittance in the skin.

In the study reported by Reichmanis *et al.* [7], an electrical model for the skin comprising a resistor in series with a parallel combination of a resistor and a capacitor was used. They found significant differences between meridian and control sites for the two resistors but not for the capacitor. In our measurements at 418 Hz, the series resistor will not contribute to the results, and the parallel resistor will hence be roughly the inverse of our measured conductance. Translating their results for the parallel resistor to conductance values, the mean value for measurements on the meridian was on average $120 \times$ SD higher than the baseline (ranging from about 2–1000 times the SD). Chen [8] also found the measured dc conductance to be more than $2 \times$ SD higher than the baseline on meridian sites. Hence, significant changes found by other investigators would have been detected with our system.

We, therefore, conclude that no line patterns were found in this study, which is in agreement with earlier studies [14].

References

[1] Ø. G. Martinsen, S. Grimnes, and O. Sveen, "Dielectric properties of some keratinised tissues—Part 1: Stratum corneum and nail *in situ*," *Med. Biol. Eng. Comput.*, vol. 35, pp. 172–176, 1997.

[2] Ø. G. Martinsen, S. Grimnes, and E. Haug, "Measuring depth depends on frequency in electrical skin impedance measurements," *Skin Res. Technol.*, vol. 5, pp. 179–181, 1999.

[3] T. Yamamoto, Y. Yamamoto, K. Yasuhara, Y. Yamaguchi, W. Yasumo, and A. Yoshida, "Measurement of low-resistance points on the skin by dry roller electrodes," *IEEE Trans. Biomed. Eng.*, vol. 35, pp. 203–209, Mar. 1988.

[4] D. Panescu, K. P. Cohen, J. G. Webster, and R. A. Stratbucker, "The mosaic electrical characteristics of the skin," *IEEE Trans. Biomed. Eng.*, vol. 40, pp. 434–439, May 1993.

[5] X. Zhu and J. K. Hao, *Acupuncture Meridian Biophysics—Scientific Verification of the First Great Invention of China* (in Chinese). Beijing, China: Beijing, 1989.

[6] M. Reichmanis, A. A. Marino, and R. O. Becker, "Laplace plane analysis of transient impedance between cupuncture points Li-4 and Li-12," *IEEE Trans. Biomed. Eng.*, vol. BME-24, pp. 402–405, 1977.

[7] M. Reichmanis, A. A. Marino, and R. O. Becker, "Laplace plane analysis of impedance on the H. Meridian," *Amer. J. Chinese Med.*, vol. 7, pp. 188–193, 1979.

[8] K.-G. Chen, "Electrical properties of meridians," *IEEE Eng. Med. Biol. Mag.*, vol. 15, no. 3, pp. 58–66, 1996.

[9] T. Yamamoto and Y. Yamamoto, "Non-linear electrical properties of the epidermal stratum corneum," *Med. Biol. Eng. Comput.*, vol. 19, pp. 302–310, 1981.

[10] Ø. G. Martinsen, S. Grimnes, and J. Karlsen, "Electrical methods for skin moisture assessment," *Skin Pharmacol.*, vol. 8, pp. 237–245, 1995.

[11] Ø. G. Martinsen and S. Grimnes, "On using single frequency electrical measurements for skin hydration assessment," *Innov. Tech. Biol. Med.*, vol. 19, pp. 395–399, 1998.

[12] S. Grimnes, "Impedance measurement of individual skin surface electrodes," *Med. Biol. Eng. Comput.*, vol. 21, pp. 750–755, 1983.

[13] T. Ragheb and L. A. Geddes, "Electrical properties of metallic electrodes," *Med. Biol. Eng. Comput.*, vol. 28, pp. 182–186, 1990.
[14] S. Grimnes, "Pathways of ionic flow through human skin in vivo," *Acta. Derm. Venereol. (Stockh.)*, vol. 64, pp. 93–98, 1984.

An Ultralight Biotelemetry Backpack for Recording EMG Signals in Moths

Pedram Mohseni*, Karthik Nagarajan, Babak Ziaie, Khalil Najafi, and Selden B. Crary

***Abstract*—A two-channel FM biopotential recording system fabricated on a foldable, lightweight, polyimide substrate is presented. Each channel consists of a biopotential amplifier followed by a Colpitts oscillator with operating frequency tunable in the 88–108 MHz commercial FM band. The overall system measures 10 mm $\times$ 10 mm $\times$ 3 mm, weighs 0.74 g, uses two 1.5-V batteries, dissipates about 2 mW, and has a transmission range of 2 m. Using this system, electromyogram signals have been recorded from the *dorsal ventral muscle* and the *dorsal longitudinal muscle* of a giant sphinx moth (*manduca sexta*).**

***Index Terms*—Biotelemetry, EMG monitor, FM transmission, manduca sexta.**

I. Introduction

Insects and other arthropods provide models for robotics in three ways: *biomimetic robots*, in which one or more structural or operational aspects of the animals are mimicked in the robot; *biohybrid robots*, in which living biological tissues up to the organ level are combined with one or more artifacts to form a robot; and *biobots*, in which an intact biological system is harnessed using applied artifacts, such as microelectronics [1]–[5]. Large and powerful insects, such as the giant sphinx moth *Manduca Sexta* or the Madagascan hissing cockroach [Blattaria, Blaberidae, *Gromphadorhina portentosa* (Schaum)] can be equipped to carry a payload, such as miniature "backpack" devices for environmental monitoring, wireless communications, or "biobotic" manipulation of behavior [6]. Male giant sphinx moths have the capability to carry loads of up to 1 g and can be used as a delivery system for a microsystem telemetry package consisting of various physical and chemical microsensors and wireless communication electronics. In addition, olfactory capabilities of these insects can be employed to generate correlative records of neural and/or muscular response to a specific chemical variable of interest [7], [8]. There is an increasing interest in monitoring the electromyogram (EMG) signals generated during the flight of these moths [9], [10]. Kuwana *et al.* recently developed a small 2-channel telemetry system for simultaneous recording and transmission of flight muscle biopotentials (EMG) [10]. The system they reported weighed 0.4–0.6 g (including battery) and had a transmission range of $\sim$1 m. In this paper, we present a simple design alternative that employs a small number of components, is frequency stable, and can be assembled in a very short time. In Section II, the recording system design and construction are described. Section III discusses the measurement results on a prototype design, and Section IV draws some conclusions from the result of this work and suggests future improvements.

Manuscript received November 16, 1999; revised February 23, 2001. This work was supported by the Defense Advanced Research Projects Agency, DARPA, under Contract N66001-98-C-OTBD. *Asterisk indicates corresponding author*.

*P. Mohseni is with the Department of Electrical Engineering and Computer Science, Center for Integrated MicroSystems, University of Michigan, 1301 Beal Avenue, room 1246 EECS, Ann Arbor, MI 48109 USA (e-mail: pmohseni@engin.umich.edu).

K. Nagarajan was with the University of Michigan, Ann Arbor, MI 48109 USA. He is now with the Maxim Corporation, Sunnyvale, CA 94086 USA.

B. Ziaie was with the University of Michigan, Ann Arbor, MI 48109 USA. He is now with the Department of Electrical and Computer Engineering, University of Minnesota, Minneapolis, MN 55455 USA.

P. Mohseni, K. Najafi, and S. B. Crary are with the Department of Electrical Engineering and Computer Science, Center for Integrated MicroSystems, University of Michigan, Ann Arbor, MI 48109 USA.

Publisher Item Identifier S 0018-9294(01)04177-5.

II. Circuit Description and Construction

Fig. 1 shows the biotelemetry backpack along with the circuit schematic of one biopotential recording and transmission channel. A simple design was selected to keep the size, weight, and power consumption as small as possible. Each channel consisted of a biopotential amplifier followed by a Colpitts transmitter with operating frequency tunable in the 88- to 108-MHz commercial FM band. A simple frequency division multiple access scheme using different transmission frequencies for each channel was considered the most suitable communication technique for a two-channel system. This technique required a small number of circuit components and did not require complex multiplexing schemes. EMG biopotential signals recorded with a wire electrode implanted inside the muscle have an amplitude and bandwidth of 1–10 mV and 100 Hz–10 kHz, respectively. Since the amplitude of the EMG signal is not high enough for direct modulation, some level of amplification is necessary. A common-source junction field effect transistor (JFET) amplifier (nominal gain $\sim$10–15) stage was used to maintain a high input impedance (1 MΩ) and a low noise figure. The amplified biopotential signal was then used to modulate a Colpitts oscillator by varying the base-collector capacitance of the oscillator transistor. Table I summarizes the values and other important characteristics of various components.

In order to reduce the weight and increase the flexibility, a thin polyimide substrate was used to fabricate the telemetry system (Dynaflex, CA). The bare substrate weighed 0.1 g and contained spiral integrated inductors (L_t) and solder-plated component assembly pads. The transmission frequency could be changed by changing this inductor. The same inductor could have been used to radiate the FM signal, but a short wire monopole antenna increased the range considerably. To reduce the number of components, all the low-value biasing resistors and coupling capacitors were integrated on an in-house fabricated resistance-capacitance (*RC*) chip. This *RC* chip contained five resistors and one capacitor. For details, see Table I. The assembly process started with mounting and wire bonding the *RC* chip to the substrate. The frequency tuning wire bonds were also performed at this stage. Next, all other passive and active surface mount components were soldered in place. This was followed by attaching the electrodes and antennae to the substrate. Fig. 2 shows a complete, fully assembled, and unfolded system. In order to mount the device on a moth, the circuit was folded in half to create a compact system. Finally, the batteries were connected to the substrate via two small stainless steel spring clips. The system was powered by two 1.5-V silver–oxide batteries, had the overall dimensions of 10 mm $\times$ 10 mm $\times$ 3 mm, and weighed 0.74 g, which is light enough to be carried by a male Manduca moth. Table I summarizes the weight

0018–9294/01$10.00 © 2001 IEEE